

NEW ADVANCES IN MOLECULAR SIEVE SCIENCE AND TECHNOLOGY

J. A. RABÓ

Union Carbide Corporation
Tarrytown, New York, U.S.A.

Received August 7, 1986

Presented by Prof. I. Szebényi

Abstract

This review gives a brief account of recent progress in molecular sieve synthesis, characterization and catalysis. The term molecular sieve, instead of zeolite, is used here with the intention to reflect the expansion of the material base from metal aluminosilicate zeolites to microporous crystals of new compositions. Completeness is not the objective of this review. The intention is, rather, to point to principal areas of progress, using representative examples from the literature.

Introduction

Progress in zeolite science and technology gained new momentum in recent years. Major advances have been achieved in the discovery of new molecular sieves, expanding the portfolio of known microporous crystals from zeolites and pure silica structures to new compositions. The characterization of microporous materials has greatly expanded, particularly by the application of solid state NMR and by improved techniques in electron microscopy and crystallography. The large family of recently discovered new crystal structures and compositions provides new opportunities in catalysis for new applications. Thirty five years after the discovery of synthetic zeolites Linde[®] A and Linde[®] X, there is no sign of maturity either in zeolite science or in technology. It seems, that this field is capable of continuous expansion both in material science and in application technology.

Synthesis of new generation molecular sieves

In this review the topic of synthesis covers both the primary synthesis work as well as important secondary chemical modifications of molecular sieve crystals. The first is the source of new crystal forms, pore structures and

* Lecture held at the Technical University of Budapest in August 1986

new chemical compositions while the latter leads to changes in composition and chemical or catalytic properties, without substantial changes in the crystal framework. In chemical modifications, preference is given to chemical substitution over thermal or hydrothermal modifications often described in the earlier literature.

Synthesis of aluminophosphate type molecular sieves

Several families of new molecular sieves based on a novel aluminophosphate family have been recently described by E. M. Flanigen, et al [1]. These materials may consist of Al and P as the only tetrahedral framework atoms (T) or they may include additional T atoms chosen from thirteen elements, with valence from one to five. These new compositions may contain up to six different T elements. The whole aluminophosphate based molecular sieve family represents more than two dozen crystal structures and about two hundred chemical compositions.

The aluminophosphate based molecular sieves are synthesized by hydrothermal crystallization from reactive aluminophosphate gels containing all framework elements and an organic template. The organic template plays a structure directing role, and upon synthesis it is incorporated in the structural voids of the crystal.

The aluminophosphate based materials are classified based on composition and crystal structure. Using the composition formula $(E1_x, Al_y, P_z) O_2$ where E1 represents one or several additional T elements, a set of acronyms have been adopted, for example, the $(Al, P) O_2$ is $AlPO_4$, the $(Si_x, Al_y, P_z) O_2$ is SAPO while more complex compositions are MeAPO, MeAPSO or EIAPSO, EIAPSO, with Me or EI representing additional T elements.

The major structures of the aluminophosphate, $AlPO_4$, based molecular sieve family represent a large variety of crystal forms including fifteen novel structures as well as several structures with topologies related to zeolite crystals, see Table 1. The structure types are identified by a number. Thus, $AlPO_4$ -5 or other $AlPO_4$ -acronyms specifically identify the chemical composition and the type of crystal structure. The numbers identifying the structure are arbitrarily chosen and they do not relate to structures used for identifying zeolites (ZSM-5, etc) or minerals. In Table 1 the important crystal forms are arranged according to pore size, showing crystals with large, intermediate, small and very small pores. It should be noted that these new molecular sieves display the whole pore size range represented by zeolites. Significantly, there are five large pore materials with pore sizes similar to large pore zeolites Y or L, and three intermediate pore materials with each representing a novel crystal form. Table 1 also gives information on the pore volume of the various

Table 1

Typical Structures in AlPO_4 —Based Molecular Sieves*

Species	Structure Type	Pore Size, nm	Saturation H_2O Pore Vol. cm^3g^{-1}	Species	Structure Type	Pore Size, nm	Saturation H_2O Pore Vol. cm^3g^{-1}
Large Pore				Small Pore (cont.)			
5	Novel, detm.	0.8	0.31	26	Novel	0.43	0.23
36	Novel	0.8	0.31	33	Novel	0.4	0.23
37	Faujasite	0.8	0.35	34	Chabazite	0.43	0.3
40	Novel	0.7	0.33	35	Levynite	0.43	0.3
46	Novel, detm.	0.7	0.28	39	Novel	0.4	0.23
Intermediate Pore				42	Linde Type A	0.43	0.3
11	Novel, detm.	0.6	0.16	43	Gismondine	0.43	0.3
31	Novel	0.65	0.17	44	Chabazitelike	0.43	0.34
41	Novel	0.6	0.22	47	Chabazitelike	0.43	0.3
Small Pore				Very Small Pore			
16	Novel			16	Novel	0.3	0.3
14	Novel, detm.	0.4	0.19	20	Sodalite	0.3	0.24
17	Erionite	0.43	0.28	25	Novel	0.3	0.17
18	Novel	0.43	0.35	28	Novel	0.3	0.21

* From: Flanigen, E. M. et al, Proceedings of the 7th International Zeolite Conference, Tokyo, Japan, August 17—22, 1986, (1)

species. It also indicates the structure type, if known, and whether the crystal structure has been determined.

The binary aluminophosphate molecular sieve family AlPO_4 exhibits constant chemical composition with an Al to P ratio of unity. This fixed composition provides electrically neutral framework structures. Consequently, there are no extra framework cations or protic acidity. The binary aluminophosphates are mildly hydrophilic, in contrast to the strongly hydrophilic zeolites and hydrophobic silica molecular sieves. The AlPO_4 crystals generally have excellent thermal and hydrothermal stability, similar to stable zeolites.

The ternary SAPO molecular sieves represent an important family of aluminophosphate based materials with a structural diversity exceeding that of the AlPO_4 materials. Here, in addition to structures also found with AlPO_4 materials, several new crystal types were synthesized with either large or intermediate pore sizes, see Table 2. If one considers the presence of silicon as a result of a T atom substitution into an aluminophosphate framework then the silicon appears mainly to replace the phosphorous. Such mechanism leads to a framework with a net negative electric charge on the (AlO_4) unit adjacent to the P deficient (TO_4) site. The consequence of such structural arrangement is the presence of exchangeable cations, which may include metal cations or H^+ . As a result of increased polarity provided by the net negative framework charge and the exchangeable cations, the SAPO materials display

Table 2

*Selected Structures and Compositions in Binary, Ternary and Quaternary Systems ^a

Structure Type	AlPO ₄	SAPO	MeAPO	(Me Elements)	MeAPSO	(Me Elements)
Large Pore						
5	X	X	X	(Co, Fe, Mg, Mn, Zn)	X	(Co, Fe, Mg, Mn, Zn)
36	—	—	X	(Co, Mg, Mn, Zn)	X	(Co, Mg, Mn, Zn)
37	—	X	—		—	
40	—	X	—		—	
46	—	—	—		X	(Co, Fe, Mg, Mn, Zn)
Intermediate Pore						
11	X	X	X	(Co, Fe, Mg, Mn, Zn)	X	(Co, Fe, Mg, Mn, Zn)
31	X	X	—		X	(Co, Fe, Mg, Mn, Zn)
41	—	X	—		—	
Small Pore						
14	X	—	X	(Mg, Zn)	—	
17	X	X	X	(Co, Fe, Mg)	X	(Co)
34	—	X	X	(Co, Fe, Mg, Mn, Zn)	X	(Co, Fe, Mg, Mn, Zn)
44	—	X	X	(Co, Mg, Mn, Zn)	X	(Co, Fe, Mg, Mn, Zn)
47	—	—	X	(Co, Mg, Mn, Zn)	X	(Co, Mg, Mn, Zn)
Very Small Pore						
20	X	X	X	(Mg)	X	(Co, Fe, Mg, Mn, Zn)

^a For elements Al, P, Si, Co, Fe, Mg, Mn, and Zn. The X designation indicates compositions and structures observed in high purity and which are well characterized.

* From: Flanigen, E. M. et al, Proceedings of the 7th International Zeolite Conference, Tokyo, Japan, August 17—22, 1986, (1)

moderate to high hydrophilic character. In addition, in the protic form all SAPO species display a wide spectrum of carboniogenic catalytic activity. The SAPO materials also show high thermal and hydrothermal stability, similar to the AlPO₄ crystals.

The other ternary and multicomponent materials may contain one or more species from a group of thirteen elements, including several transition metals. With these materials the theoretical T atom "substitution mechanism" envisioned for the incorporation of new elements is different and more complex than that envisioned for the SAPO's. Here, bi and trivalent metals seem to substitute for aluminum, giving rise to a net negative (Me²⁺) or neutral (Me³⁺) framework charge. Similar to SAPO's, these negatively charged frameworks also display ion exchange properties. They can be prepared in protic form, displaying acidic catalytic activity.

The thermal and hydrothermal stabilities of the MeAPO, MeAPSO, ElAPO and ElAPSO families identified in Tables 2 and 3 are more diverse relative to those of the AlPO₄ and SAPO families. Here, the stability depends on both chemical composition and crystal form. Many species display stability similar to AlPO₄'s and SAPO-'s while others show significantly reduced crystal

Table 3

Selected EIAPSO and EIAPSO Structures and Compositions*

Structure Type	Compositional Systems	
	EIAPSO, Elements	EIAPSO, Elements
Large Pore		
5	Be, Ca, Ge, Li, Ti	Be, Ca, Ti
36	Be, Ca	—
Intermediate Pore		
11	As, Be, Ti	As, Ge, Ti
41	—	B
Small Pore		
17	Ca, Ge	—
18	As, Ca, Ge, Ti	—
34	Be, Li	As, B, Be, Ca, Ge, Li, Ti
35	—	As, B, Ge, Ti
Very Small Pore		
20	Be, Ca, Ge, Li, Ti	Be, Ca

* From: Flanigen, E. M. et al, Proceedings of the 7th International Zeolite Conference, Tokyo, Japan, August 17—22, 1986, (1)

retentions when exposed to high temperatures or severe hydrothermal conditions.

The aluminophosphate species containing tetrahedral transition metal atoms (Co^{2+} , Mn^{2+} , $\text{Fe}^{3+,2+}$, Zn^{2+}) are of particular interest because of their potential accessibility to reactant molecules. Other compositions provide unusual examples of tetrahedral siting for Me^+ and Me^{2+} ions in an oxide lattice (Li, Mg) etc.

In addition to the large new families of aluminophosphate based molecular sieves reported from Union Carbide's laboratories, recent reports by G. C. Bond, et al [2], N. J. Tapp, et al [3] and D. R. Pyke, et al [4] also described aluminophosphate type compositions containing aluminum, phosphorous and additional elements. These molecular sieves represent ternary and occasionally quaternary aluminophosphate compositions with the -5 or the -11 type crystal structures identified in Table 1, and they contain Zn [2], Co^{2+} [3], and Si, Ti, Zn, V, Fe or Mg [4] as additional T elements. An interesting theoretical discussion on isomorphic metal substitution in molecular sieves has been also published recently by Tielen, et al [3].

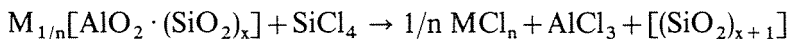
In addition to the disclosures in the scientific literature discussed above, the following US patents describe aluminophosphate based type molecular sieve compositions: US Patents $-4,310,440$, $-4,473,663$, $-4,567,029$, $-4,554,143$, $-4,440,871$, $-4,500,651$.

Synthesis of silica sodalite in non aqueous media

A new method for the synthesis of silica rich or pure silica sodalite has been reported using non aqueous synthesis media such as ethylene glycol or other suitable solvent by D. M. Bibby, [6]. The product tends to be silica rich, and in the absence of aluminum it is pure silica with unit cell composition $\text{Si}_{12}\text{O}_{24} \cdot x\text{C}_2\text{H}_4(\text{OH})_2$. Interestingly, the silica sodalite occludes no sodium containing molecules (NaOH) present in the synthesis system.

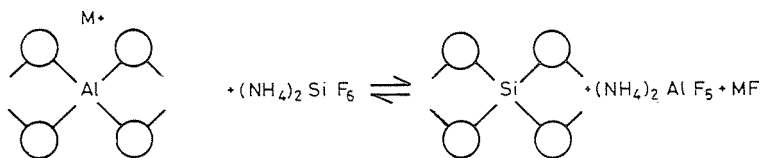
Non-destructive, post synthesis treatments

Important recent post synthesis modifications of molecular sieves involve non destructive changes in zeolite framework Si/Al ratios. Earlier it was reported by H. K. Beyer that Y zeolite can be enriched in silicon by reaction with SiCl_4 vapor:



[7]. The treatment with SiCl_4 readily results in high Si/Al ratios, yielding products showing hydrophobic character. The silicon enriched products display enhanced thermal stability, reflecting the higher stability of the Si-O versus the Al-O linkage.

More recently, a new method was described for the non destructive silicon enrichment of zeolites. According to G. W. Skeels and D. W. Breck, the replacement of zeolite framework Al atoms by Si atoms can be achieved by the application of aqueous solutions of fluorosilicate reagents at mild reaction temperatures [8]. A favored reaction scheme applied to Y zeolite is given as follows:



The overall reaction seems to proceed through two consecutive steps. It is conceived that first framework Al atoms are removed from the Y zeolite by the hydrolysed fluorosilicate solution. Subsequently, Si atoms are inserted in a slower reaction step. Rapid dealumination without silicon insertion may cause crystal collapse while the silicon-enriched products become more stable relative to the starting Y zeolite.

By appropriate choice of reaction temperature, reagent application rate and pH, it is possible to prepare Y zeolite products with $\text{SiO}_2 : \text{Al}_2\text{O}_3$ ratios

above 3 such as 10 or 20 and beyond, with high chemical efficiency and without loss in crystallinity. In the silicon enriched product, the remaining framework aluminum atoms maintain their tetrahedral coordination as indicated by $M^+ : Al$ ratios of near unity. A variety of chemical and crystallographic evidence demonstrates that the Si atoms are indeed inserted into framework sites vacated by Al atoms. For example, the material balance of the reaction system shows perfect stoichiometry between aluminum removed and inserted silicon. Crystallographic information and particularly the gradual changes in the lattice parameter a_0 observed with incremental reagent additions indicate good distribution of the inserted Si atoms throughout the Y zeolite crystal, see Table 4.

Table 4

Chemical Analyses of the Starting Zeolites and the Products of the Fluorosilicate Reaction*

	Starting NH ₄ Y	LZ-210 (9.3)	LZ-210 (14.8)	Starting H ₃ O Mordenite	LZ-211 (27.7)	NaY	Aluminum- Depleted NaY
Na ₂ O, wt.% ^a	1.88	1.04	0.61	0.21	0.10	12.4	7.2
Li ₂ O, wt.% ^a	—	—	0.37	—	—	—	—
(NH ₄) ₂ O, wt.% ^a	9.90	6.34	3.70	0	2.42	0	0
Al ₂ O ₃ , wt.% ^a	22.68	14.28	9.74	10.80	5.53	22.2	14.0
SiO ₂ , wt.% ^a	64.67	78.34	84.96	89.08	90.21	64.2	78.3
Fluoride, wt.% ^a	0	0.05	0.15	0	0.01	0	0
SiO ₂ /Al ₂ O ₃	4.84	9.31	14.84	14.00	27.70	4.92	9.52
Na ⁺ /Al	0.14	0.12	0.10	0.03	0.03	0.92	0.85
Li ⁺ /Al	—	—	0.13	—	—	—	—
NH ₄ ⁺ /Al	0.85	0.87	0.75	—	0.86	0	0
Cation Equivalent, M ⁺ /Al	0.99	0.99	0.98	0.03	0.89	0.98 ^b	0.95 ^c

^a On an Anhydrous Basis

^b Includes CaO/Al₂O₃=0.06

^c Includes CaO/Al₂O₃=0.10

* From: Skeels, G. W. et al, Proceedings of the 6th International Zeolite Conference, Reno, Nevada, July 10—13, 1983. (8)

Silicon enrichment of the Y zeolite results in major increase in thermal stability. At 60 percent replacement of the aluminum by silicon, changing the SiO₂ : Al₂O₃ ratio from ~5 to 14.8, the DTA crystal collapse temperature increases from 860°C to 1128°C, an increase of 268°C, see Table 5.

Similar to the thermal stability results, the silicon-enriched Y zeolite derivatives display greatly enhanced hydrothermal stability, relative to reference low soda Y zeolite. By comparison, following steam treatment, the low soda NH₄Y (Na₂O=0.36%) retains only ~15 percent crystallinity, while the silicon-enriched product with SiO₂ : Al₂O₃ of 11.7 retains ~90 percent crystallinity. Furthermore, the silicon enriched product with 6.4 SiO₂ : Al₂O₃ ratio already retains ~58 percent crystallinity [9].

Table 5

Physical Properties of the Starting Zeolites and the Products of the Fluorosilicate Reaction*

	Starting NH ₄ Y	LZ-210 (9.3)	LZ-210 (14.8)	Starting H ₃ O Mordenite	LZ-211 (27.7)	Na _y	Aluminum- Depleted NaY
X-Ray Crystallinity % I/I _s	100	106	93	100	106	100	68
Unit Cell. a ₀ in Å	24.67	24.49	24.39	NA	NA	24.689	24.652
Framework Infrared							
Asymmetric Stretch cm ⁻¹	1014	1044	1061	1076	1086	1019	1033
Symmetric Stretch cm ⁻¹	786	807	818	802	812	791	794
Crystal Collapse Temp by DTA °C	860	1037	1128	—	—	980	980
Hydroxyl Region Infrared							
Absolute Absorbance 3710 cm ⁻¹	0.000	0.040	0.158	0.266	0.310	0.000	0.330
O ₂ Adsorption Capacity							
90 K, 100 Torr (wt.%)	35.2	29.4	28.6	19.79	18.03	—	—
H ₂ O Adsorption Capacity							
298 K, 46 Torr (wt.%)	32.1	29.8	28.8	16.17	13.55	—	—
Neopentane Capacity							
298 K, 500 Torr (wt.%)	—	—	—	5.05	5.26	—	—

* Skeels, G. W. et al, Proceedings of the 6th International Zeolite Conference, Reno, Nevada, July 10—13, 1983. (8)

The outstanding crystal stability of framework-silicon-enriched Y products obtained by aqueous fluorosilicate treatment has been most recently again demonstrated under very severe steaming conditions by J. A. Rabo, et al. Accordingly, these materials at SiO₂/Al₂O₃ ratios greater than 6.5 display substantially superior hydrothermal stability relative to H-Y zeolite products of similar SiO₂/Al₂O₃ ratios obtained either by aluminum extraction (EDTA, acid treatment) or by steam stabilization [9].

In addition to the silicon enrichment of zeolites via post synthesis chemistry, several recent reports by M. W. Anderson, et al [10], C. D. Chang, et al [11, 12], and R. M. Dessau, et al [13] describe the aluminum enrichment of silica rich or pure silica molecular sieves. Several authors independently describe the treatment of silicalite or ZSM-5 by AlCl₃ vapor at about 400°C [10, 11, 12, 13]. Following this treatment the authors use different methods to remove excess AlCl₃ and in one case they use ion exchange technique following AlCl₃ treatment to remove aluminum incorporated as exchangeable cation [11]. It is suggested that the AlCl₃ reacts with lattice defect sites such as hydroxyl nests, presumably existing in high silica zeolites. The existence of lattice defects such as surface hydroxyls seems to be supported by the facile exchange of oxygen between zeolite and water, reported earlier [9a].

Convincing evidence for the incorporation of aluminum into tetrahedral lattice sites comes from ²⁷Al MAS NMR, and from indirect evidence such as enhanced catalytic activity [12, 13] and infrared spectroscopy. According to

the best documented ^{27}Al MAS NMR work [10], following AlCl_3 treatment of silicalite both tetrahedral and octahedral aluminum peaks are found, with about 1/3 of the aluminum in octahedral sites. The tetrahedral aluminum is presumed to occupy lattice sites while the octahedral aluminum represents extra framework cation sites. In addition to the treatment with AlCl_3 , aqueous fluoroaluminates were also applied to enrich ZSM-5 in aluminum. Here, it is proposed that aluminum insertion is not limited to lattice defects. Thus, in this case the direct substitution of framework silicon by aluminum is suggested [11].

In addition to the application of highly reactive aluminum compounds (halides), the aluminum enrichment of ZSM-5 zeolite with "aquo species from Al_2O_3 " has been also reported [12]. This involves the hydrothermal treatment of ZSM-5 and active alumina mixtures. Presumably, the hydrous alumina species migrate into the zeolite, ultimately assuming sites as framework lattice T cations. The importance of the presence of liquid water phase is emphasized, because no evidence (catalytic) for aluminum incorporation is observed by treatment in dry steam. Here again, the amount of tetrahedral aluminum is determined by ^{27}Al MAS NMR, indicating the presence of additional aluminum in the lattice following the treatment.

Recent progress in the characterization of molecular sieves

The principal areas of progress in molecular sieve characterization are NMR spectroscopy, electron microscopy, X-ray crystallography and far infrared spectroscopy.

Nuclear magnetic resonance, NMR, spectroscopy

It is fortunate for zeolite science that in recent years this topic attracted the attention of several leading NMR spectroscopists. The reason for interest was the opportunity to apply solid state NMR, using the MAS and a series of other sophisticated techniques, to characterize the adjacent T atom environment of framework T atoms in zeolites. This information was especially desirable because X-ray techniques do not readily distinguish Si from Al atoms, and because the interpretation of zeolite chemistry and catalysis rests upon the relationship and distribution of T atoms in the zeolite matrix. The most broadly applicable investigations deal with MAS NMR of ^{29}Si and ^{27}Al , and with the characterization of acidic hydrogen atoms. An independent area of NMR investigation is the use of xenon as a probe in the study of zeolites.

In the studies of zeolite T atoms by NMR interest was attached to check the validity of Lowenstein's rule which forbids the existence of two more Al atoms at adjacent T sites. This rule rests on the reasonable assumption that the net negative charge on tetrahedral alumina units would destabilize similar units at adjacent sites, and on the information that zeolite and silicate chemistry is fully consistent with this rule. The ^{29}Si and ^{27}Al MAS NMR has been applied to test and to verify this structural rule for Al. After considerable investigation and debate, it has been shown by J. M. Bennett, et al that recent MAS NMR evidence with zeolites is fully consistent with Lowenstein's rule [14]. Thus, the existence of twin, adjacent tetrahedral alumina units is excluded from structural considerations.

Important and informative structural information for zeolites has been provided by ^{29}Si MAS NMR spectroscopy by C. A. Fyfe, et al [15, 16], J. Klinowski [17, 18], J. M. Thomas [19] and by C. S. Blackwell [14]. Here, with the ability to distinguish between Si sites with 0, 1, 2, 3 or 4 adjacent Al atoms, an opportunity developed to characterize the zeolite lattice, for example to:

- Distinguish between all five Si species with 0, 1, 2, 3 and 4 Al atoms at adjacent sites, see Fig. 1.
- Distinguish between different structural sites for Si.
- Calculate the Si/Al ratio of the zeolite crystal framework.

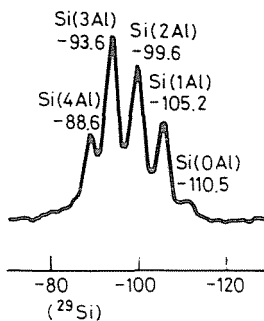


Fig. 1. ^{29}Si -MAS-NMR spectrum at 79,8 MHz of zeolite ZK-4 showing five peaks, at the chemical shift values indicated, corresponding to the silicon environments shown in the figure (from: Fyfe, C. A. et al, *Angewandte Chemie*, (April, 1983) p. 272. [16])

In the case of Y zeolite with a single crystallographic T atom lattice site, the characterization of T atoms adjacent to Si allows the monitoring of important structural and chemical changes occurring in zeolite framework. This method can follow the framework dealumination process occurring in the steaming of H-Y zeolite. Here, while chemical analysis shows no change, the ^{29}Si MAS-NMR reveals the silicon enrichment, showing more Si with higher number of Si atoms at adjacent sites, see Fig. 2.

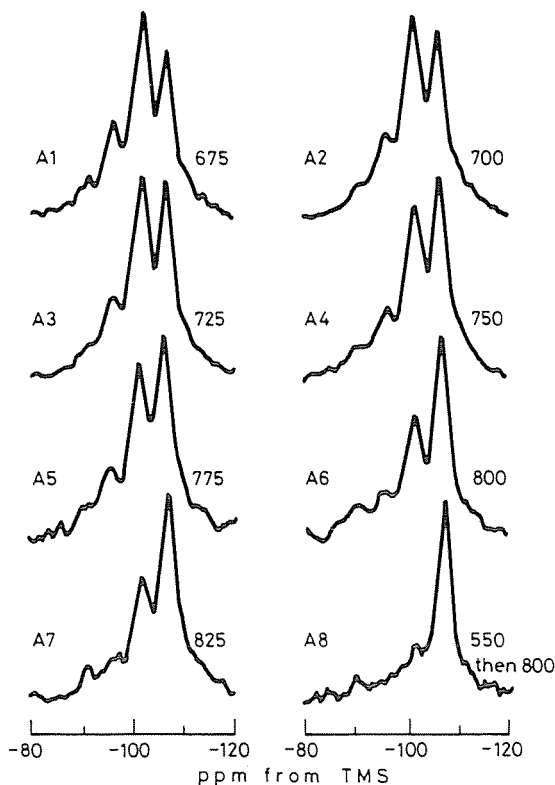


Fig. 2. ^{29}Si -MAS-NMR spectra of hydrothermally dealuminated samples. Temperatures in $^{\circ}\text{C}$ (from: Klinovski, J. et al, *J. Chem. Soc.* (1985) pg. 3011. [18])

Al MAS NMR also substantially contributed to the elucidation of the siting of Al both in as-synthesized zeolites and in steamed or chemically modified products. The most important aspect of Al characterization is the quantitative determination of its tetrahedral vs octahedral coordination, see Fig. 3. Since pure alumina phases prefer octahedral Al coordination it is expected that non framework Al prefers octahedral sites. Thus, the determination of tetrahedral vs octahedral Al provides information on the Al in the zeolite framework and for the determination of the framework Si/Al ratio. In addition, it reveals the formation of extra framework alumina phases formed upon steaming or following other chemical treatment [15, 16, 17, 18, 19].

Combined ^{29}Si and ^{27}Al MAS NMR yields quantitative information on as-synthesized zeolite crystals. However, in certain cases the quantitative interpretation on Al T atoms can become difficult because of line broadening, caused by interaction of the Al quadrupole moment with the adjacent electric field in the crystal. This problem can be further aggravated by non symmetrical electron distribution surrounding the Al atom. Attempts to quantify all Si

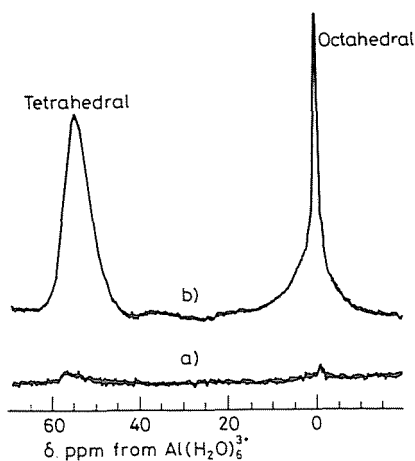


Fig. 3. ^{27}Al -MAS-NMR spectra at 104.22 MHz of the parent and the aluminated ZSM-5 silicalite. 500 Scans with no line broadening. (a) Parent material with Si : Al 400. (b) aluminated material (see text) with Si : Al ca. 50. (from Anderson, M. W. et al, *J. Chem. Soc.*, (1984), pg. 1596 [10])

and Al information further suffers in the presence of lattice defects such as OH groups attached to T atoms. While NMR techniques such as “cross polarization” identifies hydroxylated species, the quantitative assessment of these species remains a difficult task. Thus, the presence of defect sites such as hydroxyl, frequently present in zeolites, renders quantitative characterization of the lattice of practical zeolite catalysts difficult.

A particularly important aspect of NMR studies relates to the characterization of acidic hydrogen atoms attached to framework oxygen atoms. A recent investigation by H. Pfeifer [20] directed to zeolite acidity applied extensive experimental and theoretical studies to both Si, and Al as well as to H atoms, comparing silica-alumina gel, H-mordenite and H-Y zeolites [20]. An interesting experimental aspect of the study is the application of a MAS sample holder device which can be sealed to render it applicable for proton MAS NMR studies. Important conclusions of this proton and ^{27}Al MAS NMR study are that upon dehydroxylation of H-Y there is no evidence for the formation of significant amounts of 3-coordinated Al, and that the number of bridging OH groups and of 4-coordinated Al are equal, and finally that much less than half of the original 4 coordinated Al remains when dehydroxylation is complete. Surprisingly, the study of acidic hydrogen shows similarity between the acidic H species found either in silica-alumina gel, H mordenite or in H-Y zeolite; they are all found at about 4–5 ppm. The similarity (in ppm) of the acidic H species leads the author to conclude that “the higher catalytic activity of H-Y zeolites and H-mordenites with respect to amorphous silica-aluminas is due to the higher amount of acidity

(concentration of Bronsted sites) and not due to a special type of acidity" [20]. This conclusion is unexpected, and it is in opposition to the vast body of physical, chemical and catalytic data published on this topic. The latter evidence supports the conclusion that protic acid sites in H-mordenite and H-Y zeolites are intrinsically stronger relative to similar sites in silica-alumina gel. Clearly, there is a need for further investigation to explain these unexpected proton NMR data.

A new, interesting field is the NMR study of zeolites using adsorbed xenon as a probe developed by J. P. Fraissard, et al [21, 22, 23]. The concept is to apply a non-reactive molecule, particularly sensitive to its environment and to collisions with other chemical species, which could serve as a probe for determining properties of solid catalysts, especially zeolites. The probe chosen (xenon) must be detectable by NMR since this technique is particularly suitable for the detection of electron perturbations in rapidly moving molecules.

In summary, the Xenon NMR technique provides new, important information on:

- The degree of short range crystallinity in the zeolite lattice.
- The existence of cavities and channels in the same sample. It is also possible to determine whether or not they are interconnected.
- The approximate dimensions of pores in a zeolite of unknown structure.
- The locations of strongly chemisorbed molecules, for example in the channels or in the side pockets of mordenite.
- The relative value of the local electric field in the cavities and channels.

With metal loaded zeolites this technique can determine the quantitative distribution of molecules chemisorbed on the metal particles, the number of particles in the sample and, consequently, the average number of atoms per metal particle. It can also determine quantitatively the distribution of several gases simultaneously chemisorbed on these encaged particles and can be used to calculate the percentage of metal located inside or outside the zeolite crystallites.

With the emergence of molecular sieves of new compositions such as the aluminophosphate family the structural complexity of the molecular sieve lattice has been greatly increased. For reasons discussed above, with these new materials the various NMR techniques are expected to play a dominant role [14], to complement X-ray and other techniques in the characterization of the atomic order in the molecular sieve lattice.

Electron microscopy

Electron microscopy has been improved in resolution. This is mainly the result of combination with crystallographic information and computer techniques, resulting in a highly refined method to visualize structural details of zeolites such as lattice defects, intergrowth as well as the micropores themselves at near atomic level. The successful integration of information from several independent sources to attain reiterative refinement is important development in electron microscopy, and it also inspires the adoption of similar interacting techniques in other areas of crystal characterization. Excellent summaries on progress in this field has been recently published by J. M. Thomas, a major contributor to this field [19].

Progress in crystallography

Certain natural zeolites are found in crystal sizes well exceeding 100 micron in all dimensions, providing good opportunity to collect adequate X-ray diffraction information for accurate electron density maps, and to allow the definition of the crystal lattice with high degree of reliability. There are intrinsic problems in this crystallography with molecular sieve crystals such as the large unit cell size, often combined with high symmetry (Y zeolite) and with fractional occupation of certain crystallographic sites (cations). In addition, the presence of atoms at low coordination and/or low symmetry gives rise to high thermal vibrational amplitudes, all reducing the quality of the experimental data set. The problems cited above are further aggravated with crystals containing lattice defects such as those obtained upon steaming or other chemical treatments. For these reason, the efficiency of the structure refinement programs applied locating atomic positions is of great importance.

In order to improve structure refinement, a new program package was designed by Baerlocher, et al [24, 25, 26] for X-ray powder diffraction data, capable of refining structures with more than 100 structural parameters. First, a standard peak-shape function is determined from the observed profile. Then, in order to supplement the diffraction data, known interatomic distances and angles are applied as weighted constraints and their expected range is imposed as boundary condition. This method enhances the least-squares convergence, and substantially contributes to the refinement of complex structures. The application of these "soft restrictions" on bond distances and angles in the structure refinement program facilitated locating extra framework atoms which would have been missed otherwise [24, 25, 26].

Interesting structural phenomena has been recently reported by A. Alberti regarding phase transitions in zeolites [27]. Some zeolites show heat-induced phases stable over a long period of time. This stability is a consequence of the breaking of T-O-T bridges, causing topological changes in the framework. In some cases the framework of the heat-induced phase is topologically the same as that of a known mineral. Topological changes are explained on the basis of extra framework cation movements, causing strain on the T-O-T bridges. The strain facilitates proton attack, and the consequent breaking of these bonds. This process occurs only when water is present. The behavior of zeolites on heating may be arranged in the following categories [27].

- Dehydration with rearrangement of extraframework cations without considerable changes in the geometry of the framework and in the cell volume. Zeolite A, faujasite, natural chabazite and mordenite are examples of this thermal behavior.
- Dehydration with considerable distortion of the framework and a decrease in the cell volume, followed by fast rehydration and reversion of the structure at room conditions. Natrolite has a thermal behavior of this type.
- Dehydration with topological changes of the framework as a consequence of the breaking of T-O-T bridges. Examples of this behavior are: barrerite, stellerite, heulandite and zeolite EAB.

These crystallographic studies are very relevant to other aspects of zeolite chemistry such as steam induced transformations in the zeolite lattice.

Far-infrared spectroscopy

Far-infrared spectroscopy extensively developed by G. A. Ozin and associates is a fast growing contributor to the field of molecular sieve characterization [28]. It is an ideal technique for probing the vibrations of the zeolite framework occurring between 250 and 400 cm^{-1} , as well as those of cations and occluded metal atoms or clusters with frequencies between 250 and 30 cm^{-1} . While the method is not new [29], recently it has been intensively pursued and extended. This technique can identify zeolite cations, and distinguish each cation sited at different crystallographic sites, see Fig. 4. It has been also successfully applied to characterize silver clusters occluded in A zeolite. Interestingly, with silver clusters increasing in size from 2 to 10 atoms the Ag-Ag frequency shows a continuous shift to a lower cm^{-1} value. Far infrared spectroscopy is also applicable to locate transition metal cations in zeolites. A comprehensive recent review of this field is also available [28].

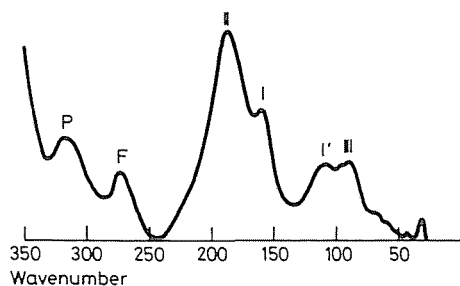


Fig. 4. The far-IR absorbance spectrum of fully dehydrated Na.Y (recorded in our laboratory). P denotes a pore opening mode and F an oxygen framework vibration. (from: Baker, M. D. et al, Catal. Rev.—Sci. Eng. (1985) p. 598. [28])

New advances in molecular sieve catalysis

Progress in molecular sieve catalyst technology is best reflected by the large variety of molecular sieve types and applications described in the literature. Rapid growth is also indicated by the commercial success of molecular sieve based catalysts. At present, in terms of sales value, about fifty percent of all heterogeneous catalysts applied in the industry contain molecular sieve as key component. The industrially relevant new applications use a variety of new generation molecular sieves as well as new modifications of known zeolites.

Catalytic cracking

In the catalytic cracking process catalysts based on zeolite Y or its modified derivatives continue to dominate. Significant advances have been made recently to respond to market needs for higher gasoline octane, and higher catalyst stability, particularly for the treatment of residual feedstocks.

An important recent catalyst development is related to the non destructive framework substitution of Si for Al in the Y zeolite, described in Chapter 2 [8]. Using this recently disclosed mild aqueous chemistry, silicon enriched forms of the Y zeolite structure have been synthesized, called LZ-210, greatly improving the thermal and hydrothermal stability of the Y crystal. Catalytic cracking catalysts prepared from these silicon rich zeolites show substantially increased cracking activity retention, following severe steaming pretreatments. In addition, finished catalysts using this zeolite show improved gasoline yield and higher coke selectivity. It has been reported that with these catalysts the production of high octane gasoline can be achieved without the usually observed impairment in gasoline yield [9]. The high activity retention and

high selectivity of these catalysts is interpreted by G. N. Long, et al. [30] on the basis that these zeolites have less aluminum and more silicon atoms in the crystal at the start of catalyst preparation. Therefore, upon steaming and concurrent hydrolysis of framework aluminum atoms these crystals develop less defect sites and less intracrystalline voids, formed from coalescent defect sites. Since defect sites contribute to the crystal decomposition rate, silicon enriched crystals are expected to lose crystallinity at a slower rate than the aluminum rich variety which has higher defect site concentration. The higher selectivity is explained on the basis that with the silica rich crystals the amount of occluded amorphous silica-alumina debris formed upon steaming is reduced. With a higher fraction of selective zeolite acid sites, and less occluded "debris acid" sites, recognized for low selectivity in cracking, higher gasoline and coke selectivity is expected, relative to H-Y zeolites [9, 30].

Another interesting effort in catalytic cracking is the application of ZSM-5 zeolite as an octane boost catalyst additive. [31, 32, 33]. Reportedly, even small amounts of ZSM-5 can readily increase the gasoline octane by several octane units. However, the octane enhancement coincides with gasoline yield loss, with up to two percent yield loss for each octane unit gained. Such application may be warranted if the ultimate refinery gasoline yield loss can be minimized by recycling the excess C_3 — C_4 olefins and the isobutane formed on ZSM-5, via alkylation process. Thus, an excess alkylation capacity is essential here for satisfactory process economy.

Aromatization of hydrocarbons

The dehydrocyclization of n-hexane over platinum loaded alkali L zeolite earlier reported by J. R. Bernard [31] became the subject of recent industrial development [35]. In contrast to the acidic commercial reforming catalyst the new L zeolite catalyst reported by T. R. Hughes, et al [35] is non acidic Pt-BaK-L zeolite. Presumably, this catalyst uses only the properties of platinum clusters for catalytic action. The catalyst is extremely sensitive to sulfur, but using thoroughly desulfurized feed one year long run has been successfully completed with refinery light naphtha.

In the dehydrocyclization of paraffins the non acidic Pt-BaK-L catalyst shows remarkable activity and selectivity advantage over the commercial, acidic reforming catalysts, see Fig. 5 and Table 6. With n-hexane the reaction rate advantage is eightfold. With higher carbon number paraffins the rate advantage is declining. However, even with n-nonane feed a modest rate advantage is observed over the acidic catalysts. The aromatization selectivity of the L zeolite catalyst is very high (82—90) and approximately constant for C_6 — C_9 n paraffins. In contrast, the selectivity of the acidic catalysts is lower, and it increases in the same carbon number range from 26 to 68 percent.

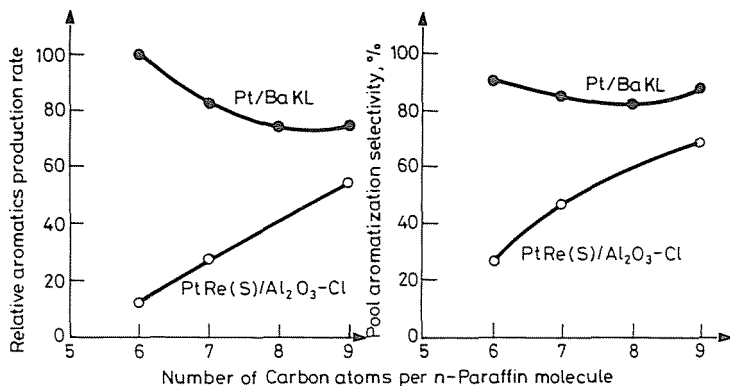


Fig. 5. Effect of number of carbon atoms per molecule on rate and selectivity of aromatization of n-paraffins at 766 K and 18 LHSV. (from: Hughes, T. R. et al, Proceeding of the 7th International Zeolite Conference, Tokyo, Japan, August 17—22, 1986, to be published. [35])

In the aromatization of alkylcyclopentanes the Pt-BaK-L catalyst is nearly as active and selective as the acidic commercial catalysts. It is proposed that the efficiency of this catalyst in this reaction is related to the non selective cyclic mechanism proposed earlier by Gault and associates, [36] which is also consistent with the nonequilibrium distribution of methylheptane isomers from the conversion of n-octane over the Pt-BaK-L catalyst, see Table 6.

Table 6

Conversion of N-Octane over Monofunctional and Bifunctional Platinum Catalysts ^a *			
	0.8 Pt/Ba KL-866	0.6 Pt/Al ₂ O ₃ -Cl	Equilibrium
C ₈ aromatics (moles/100 moles n-octane)	30	16	—
C ₈ -aromatics isomer distribution			
ethylbenzene and o-xylene	88	63	32
m- and p-xylene	12	37	68
Methylheptane isomer distribution			
2-methylheptane	8	31	36
3-methylheptane	34	47	48
4-methylheptane	58	22	16

^a Reaction conditions: 733 K, 6 LHSV.

* Hughes, T. R. et al, Proceedings of the 7th International Zeolite Conference, Tokyo, Japan, August 17—22, 1986, (35)

*Catalysis with silicoaluminophosphate molecular sieves**Conversion of methanol to C₂—C₄ olefins*

Highly selective conversion of methanol to light (C₂—C₄) olefins has been reported by S. W. Kaiser [37] using silicoaluminophosphate (SAPO) molecular sieves described in Chapter 2. With the small pore SAPO-34 catalyst the combined molar selectivities to light olefins total up to 96% at ~100 percent methanol conversion, using practical reaction conditions [37]. Increasing reaction temperatures result in increased ethylene selectivity, achieving over 60 percent ethylene selectivity at 450°C, see Table 7. The methane formation from methanol is very low at all reaction conditions. The SAPO-34 catalyst is readily regenerable via air activation and it shows good durability upon extended use. The SAPO-34 converts not only methanol but also higher alcohols, aldehydes, methyl formate and other oxygenates to mixtures of C₂—C₄ olefins. The similarity of the olefin product composition obtained with these different feeds suggests the existence of similar product precursors in the reaction chain.

Table 7

SAPO-34 *		
	375°C	450°C
Ethylene	43.0	61.1
Ethane	0.5	0.7
Propylene	41.8	27.4
Propane	0.5	0.0
Butenes	10.8	5.4
C ₅	1.7	0.6
C ₆	0.0	0.0
Methane	1.3	4.8
C ₂ -C ₄ Olefin eff.	95.6	93.9
Run time, Hr	5.2	11.0
Feed	70/30 H ₂ O/CH ₃ OH (Weight)	
WHSV	ca. 2.8 Hr ⁻¹	
CH ₃ OH Conv.	100%	

* From: Kaiser, S. W., "Silicoaluminophosphates Molecular Sieves, C₂-C₄ Olefin Formation", 1985. (37)

Reactions of aromatics using silicoaluminophosphate molecular sieves

The alkylation of toluene by methanol using silicoaluminophosphate molecular sieves has been recently described by R. J. Pellet, et al [38]. A variety of these molecular sieves with medium ($\sim 6\text{\AA}$) and large pores ($\sim 8\text{\AA}$) have been tested together with a ZSM-5 structure type zeolite LZ-105 used as reference. The results show that the LZ-105 zeolite catalyst has higher activity relative to the SAPO catalysts. However, the near 100 percent alkylation selectivity of the medium pore SAPO-11 and SAPO-31 versus the methyl group disproportionation reaction is maintained in a much larger temperature range relative to the LZ-105. Furthermore, the medium pore SAPO catalysts and particularly the SAPO-11 show "para selectivity", well exceeding the equilibrium concentration for this isomer in the product. Under similar conditions, the LZ-105 catalyst produces para xylene only at equilibrium concentration.

The catalytic tests also show that the medium pore SAPO's show much superior methylation selectivity relative to the large pore SAPO-5 catalyst. This latter molecular sieve shows very high methyl group disproportionation selectivity similar to the performance of LZ-105 catalyst at comparable temperature [38], see Table 8.

Table 8

Toluene Methylation with SAPO Molecular Sieves ^a *

Molecular Sieve Type	SAPO-5	SAPO-11	SAPO-31	SAPO-40	SAPO-41	LZ-105	LZ-105
Pore Size, Å	8	6	7	7	6	6	6
Temperature °C.	425	425	425	425	425	425	315
Pressure, psig	100	100	100	100	100	100	100
WHSV, g-1	5.6	5.6	5.6	5.6	5.6	5.6	21.0
Initial Catalyst Performance ^b							
Toluene Conversion, %	46.5	56.2	29.2	5.7	15.6	55.8	19.0
Methylation Selectivity ^d , %	41.3	99.7	97.7	99.7	98.1	21.9	99.7
Disproportionation Selectivity ^c , %	58.7	0.3	2.3	0.3	1.9	78.1	0.3
Para Isomer in Xylene, %	22.6	48.6	34.7	30.6	31.4	23.8	25.7

^a Feed composition 67 vol% Toluene + 33 vol% Methanol.

^b Initial performance was obtained by linear regression of data collected during typical 5 hour runs, extrapolated to time = 0.

^c Disproportionating selectivity is given by $2X$ (moles benzene yield)/(moles toluene converted) X100 and assumes 2 toluene \rightarrow 1 benzene + 1 xylene.

^d Methylation selectivity = 100-disproportionation selectivity.

* From: Pellet, R. J. et al, Proceeding of the 7th International Zeolite Conference, Tokyo, Japan, August 17-22, 1986, (38)

The isomerization of xylenes has been described in another publications using SAPO-5 type crystals which have been synthesized with compositions consisting of aluminum phosphorous and in several cases additional elements including Ti, Mg, Zn and Fe [4]. The data show that these large pore materials have catalytic activity for the isomerization of xylene mixtures.

Oligomerization of small olefins with silicoaluminophosphates molecular sieves

Medium pore silicoaluminophosphates have high activity and high selectivity for the oligomerization of propylene to isohexenes, producing only minor amounts of C₉ isomers [38]. The results in Table 9 demonstrate strong catalyst pore size and acid strength effects in this reaction. The large pore SAPO-5 presumably produces large oligomerizates which plug the pores and rapidly deactivate this catalyst. Conversely, the small pore SAPO-34 is active for the conversion of propylene; however, it is incapable of forming significant quantities of gasoline range oligomerizate due to its small pore size. Of the molecular sieves tested only the medium pore materials, SAPO-11, SAPO-31 and the LZ-105 type zeolite used as reference, are effective for the oligomerization of propylene. However, here too, different degrees of molecular sieving effects are indicated by the produced liquid product boiling above 215°C. Clearly, the LZ-105 zeolite produces heavier products than either SAPO-11 or SAPO-31 molecular sieves, suggesting slightly larger pore size for this

Table 9

Vapor Phase Propylene Oligomerization *

Molecular Sieve	SAPO-5	SAPO-11	SAPO-31	SAPO-34	LZ-105
Pore Size, Å	8	6	7	4.3	6
Run Temperature	700	700	700	700	703
Pressure, psig	25	25	50	25	25
Time on Feed, hrs	4.3	4.2	5.5	2.33	3.5
C ₃ = WHSV, g - l	0.98	0.94	1.04	0.53	0.90
C ₃ = Conversion, %	0	86.3	76.2	41.6	81.6
C ₅ + Selectivity, % ^a	—	77.0	82.7	19.5	37.2
Liquid Product					
Refractive Index	—	1.43	1.43	—	1.52
215°C + Fraction of					
Liquid Product, %	—	8	10	—	20

^a C₅ + Selectivity = (C₅ + yield, wt%)/(C₃ = conversion, wt%) X100.

* From: Pellet, R. J. et al., Proceedings of the 7th International Zeolite Conference, Tokyo, Japan, August 17—22, 1986, (38)

zeolite catalyst. These results are consistent with the toluene methylation study described above where the zeolite catalyst exhibited no para xylene selectivity, in contrast to the medium pore SAPO's.

The influence of acid strength on oligomerization selectivity is also apparent from the data in Table 9, and they confirm earlier reports on the mild acid character of the SAPO molecular sieves. While the SAPO-11, SAPO-31 and the reference zeolite catalyst are all medium pore molecular sieves, the SAPO materials produce more olefin rich products relative to that obtained with the zeolite. Correspondingly, the products produced by the zeolite catalyst are rich both in aromatics and light paraffins. In contrast, the SAPO-11 and SAPO-31 catalysts have significantly lower hydrogen transfer activity relative to the zeolite reference, resulting in much higher selectivity to liquid olefin products.

References

1. FLANIGEN, E. M.—LOK, B. M.—PATTON, R. L.—WILSON, S. T.: Proceedings of the Seventh International Zeolite Conference, Tokyo, Japan, August 17–22, 1986.
2. BOND, G. C.—GELSTHORPE, M. R.—SING, K. S. W.—THEOCHARIS, C. R.: "Incorporation of Zinc in an Aluminophosphate Microporous Phase", *J. Chem. Soc., Chem. Commun.*, 1056 (1985).
3. TAPP, N. J.—MILESTONE, N. B.—WRIGHT, L. J.: "Substitution of Divalent Cobalt into Aluminophosphate Molecular Sieves", *J. Chem. Soc., Chem. Commun.*, 1801 (1985).
4. PYKE, D. R.—WHITNEY, P.—HOUGHTON, H.: "Chemical Modification of Crystalline Microporous Aluminum Phosphates", *Applied Catalysis*, *18*, 173 (1985).
5. TIELEN, M.—GEELLEN, M.—JACOB, P. A.: "Isomorphic Substitution in Zeolites: Its Potential Catalytic Implications". *Proc. Zeolite Symposium Siófok, Hungary, 1985*, 8.
6. BIBBY, D. M.—DALE, M. P.: "Synthesis of Silica-Sodalite from Non-Aqueous Systems", *Nature*, *317*, 157 (1985).
7. BEYER, H. K.—BELENYKAGA, I.: *New Method for the Dealumination of Faujasite-Type Zeolite, Catalysis by Zeolites*, Elsevier, 203 (1980).
8. SKEELS, G. W.—BRECK, D. W.: "Zeolite Chemistry V—Substitution of Silicon for Aluminum in Zeolites via Reaction with Aqueous Fluorosilicate", *Proceedings from the Sixth International Zeolite Conference, Reno, Nevada, July 10–15*, 87 (1984).
9. RABÓ, J. A.—PELLET, R. J.—MAGEE, J. S.—MITCHELL, B. R.—MOORE, J. W.—LETZSCH, W. S.: "High Stability Zone Zeolites in Octane Catalysts—New Products from Union Carbide Corporation and Katalistiks International, Inc.", *Proceedings from the 1986 NPRA Annual Meeting, Los Angeles, California, March 23–25*, 1986.
- 9a. RABÓ, J. A.: "Speculations on Molecular Sieve and Isomerization Effects on Y Zeolites", *Proc. 6th International Zeolite Conf.*, 41 (1984).
10. ANDERSON, M. W.—KLINOWSKI, J.—XINSHENG, L.: "Alumination of Highly Siliceous Zeolites", *J. Chem. Soc., Chem. Commun.* 1596 (1984).
11. CHANG, C. D.—CHU, C. T. W.—MIALE, J. N.—BRIDGER, R. F.—CALVERT, R. B.: "Aluminum Insertion into High Silica Zeolite Frameworks. Reaction with Aluminum Halides", *J. Am. Chem. Soc.*, 8143 (1984).
12. CHANG, C. D.—HELLRING, S. D.—MIALE, J. N.—SCHMITT, K. D.: "Insertion of Aluminum Into High-Silica-Content Zeolite Frameworks", *J. Chem. Soc., Faraday Trans. I.* 2215 (1985).

13. DESSAU, R. M.—KERR, G. T.: "Aluminum Incorporation into High Silica Zeolites": *Zeolites*, **4**, 315 (1984).
14. BENETT, J. M.—BLACKWELL, C. S.—COX, D. E.: *J. Phys. Chem.*, **87**, 3785 (1983) and **87**, 5050 (1983).
—SMITH, J. V.—BLACKWELL, C. S.: "Nuclear Magnetic Resonance of Silica Polymorphs", *Nature*, **303**, 19 May 1983.
—BLACKWELL, C. S.—PLUTH, J. J.—SMITH, J. V.: "The Silicon/Aluminum Ratio of Single Crystals of Zeolite A Used for Crystal Structure Analysis", *J. Phys. Chem.*, **89**, 4420 (1985).
—BLACKWELL, C. S.—PATTON, R. L.: "Aluminum-27 and Phosphorous-31 Magnetic Resonance Studies of Aluminophosphate Molecular Sieves", *J. Phys. Chem.*, **88**, 6135 (1984).
15. FYFE, C. A.—GOBBI, G. C.—KENNEDY, G. J.—GRAHAM, J. D.—OZUBKO, R. S.—MURPHY, W. J.—BOTHNER-BY, A.—DADOK, J.—CHESNICK, A. S.: "Detailed Interpretation of the ^{29}Si and ^{27}Al High-Field MAS NMR Spectra of Zeolites Offretite and Omega", *Zeolites*, **5**, 179 (1985).
16. FYFE, C. A.—THOMAS, J. M.—KLINOWSKI, J.—GOBBI, G. C.: "Magic-Angle-Spinning NMR (MAS NMR) Spectroscopy and the Structure of Zeolites", *Angewandte Chemie*, **22**, 259 (1983).
17. KLINOWSKI, J.: "Nuclear Magnetic Resonance Studies of Zeolites" *Progress in NMR Spectroscopy*, **16**, 237 (1984).
18. KLINOWSKI, J.—FYFE, C. A.—GOBBI, G. C.: "High-Resolution Solid State Nuclear Magnetic Resonance Studies of Dealuminated Zeolite Y", *J. Chem. Soc. Faraday Trans.* **3003** (1985).
19. THOMAS, J. M.: "New Approaches to the Structural Elucidation of a Zeolite and Related Catalysts", *Proc. of the 8th International Congress on Catalysis*, **1**, 31 (1984).
THOMAS, J. M.: "High Resolution Electron Microscopic and Optical Diffractometric Studies of Zeolites", *Proc. of the 6th International Zeolite Conference*, 793 (1982).
20. PFEIFER, H.—FREUDE, D.—HUNGER, M.: "Nuclear Magnetic Resonance Studies on the Acidity of Zeolites and Related Catalysts", *Zeolites*, **5**, 274 (1985).
21. FRAISSARD, J. P.—ITO, T.—DE MENORVAL, L. C.: "Nuclear Magnetic Resonance Study of Xenon Adsorbed on Zeolites and Metal-Zeolites. Application to Catalysis Research." *Proceedings of the 8th International Congress on Catalysis, Berlin 25* (1984).
22. SPRINGUEL-HUET, M. A.—ITO, T.—FRAISSARD, J.: "Adsorption of Xenon: A New Method for Studying the Crystallinity of Zeolites", *Structure and Reactivity of Modified Zeolites*, **13** (1984).
23. ITO, T.—DE MENORVAL, L. C.—GUERRIER, E.—FRAISSARD, J. P.: "NMR Study of ^{129}Xe Adsorbed on L, Z and ZSM Zeolites", *Chem. Phys. Lett.*, **271** (1984).
24. BAERLOCHER, CH.: *The X-ray Rietveld System*, Institut fuer Kristallographie Petrographie, ETH, Zurich, (1982).
25. BAERLOCHER, CH.—HEPP, A.: "A New Pattern Fitting Structure Refinement Program for X-Ray Powder Data", *Proceedings of Symposium on Accuracy in Powder Diffraction*, NBS, Gaithersburg, MD, June 11–15, 165 (1980).
26. MCCUSKER, L. B.—BAERLOCHER, C.—NAWAZ, R.: "Rietveld Refinement of the Crystal Structure of the New Zeolite Mineral Gobbinsite" *Z. für Kristallographie*, **171**, 281 (1985).
27. ALBERTI, A.—VEZZALINI, G.: "Topological Changes in Dehydrated Zeolites: Breaking of T-O-T Bridges", *Proc. 6th International Zeolite Conference*, 834 (1984).

28. BAKER, M. D.—OZIN, G. A.—GODBER, J.: "Direct Probe Fourier Transform Far-Infrared Spectroscopy of Metal Atoms, Metal Ions and Metal Clusters in Zeolites", *Catal. Rev.-Sci. Eng.*, 591–651 (1985).
29. BRODSKII, I. A.—ZHDANOV, S. P.—STANEVIC, A. E.: *Opt. Spectrosc.*, 58 (1971).
30. LONG, G. N.—CHIANG, R. L.—PELLET, R. J.—RABÓ, J. A.: "New Union Carbide Framework Silicon Enriched Molecular Sieves for FCC Applications", *Proceedings of the Katalistiks' 7th Annual Fluid Cat Cracking Symposium, Venice, Italy, May 12 and 13, 1986.*
31. MAGEE, J. S.—CORMIER, W. E.—WOLTERMANN, G. M.: "Octane Catalysts Contain Special Sieves", *Oil and Gas Journal Report* 63–64 (1985).
32. VAN DIJK, J.—RAWLENCE, D. J.: "FCC Technology", Presented at the International Symposium on Zeolites For Industry, Manchester, England, April 3–5, 1984.
33. CHESTER, A. W.—CORMIER, W. E.—STOVER, W. A.: "Octane and Total Yield Improvement in Catalytic Cracking", U. S. Patent 4,309,279, (1982).
34. BERNARD, J. R.: *Proceedings of the Fifth International Conference on Zeolites, Heyden, London, p. 686 (1980).*
35. HUGHES, T. R.—BUSS, W. C.—TAMM, P. W.—JACOBSON, R. L.: *Proceedings from the Seventh International Zeolite Conference in Tokyo, Japan, August 17–22, (1986). To be published.*
36. BARRON, Y.—CORNET, D.—MAIRE, G.—GAULT, F. G.: *J. Catal.*, 152 (1963).
MAIRE, G.—POOUIDY, G.—PRUDHOMME, J. C.—GAULT, F. G.: *J. Catal.*, 556 (1965).
BARRON, Y.—MAIRE, G.—MULLER, J. M.—GAULT, F. G.: *J. Catal.* 428 (1966).
37. KAISER, S. W.: "Methanol Conversion to Light Olefins over Silicoaluminophosphate Molecular Sieves", *The Arabian Journal for Science and Engineering*, 361 (1985).
38. PELLET, R. J.—LONG, G. L.—RABÓ, J. A.: *Proceedings of the Seventh International Zeolite Conference, Tokyo, Japan, August 17–22, (1986). To be published.*

Dr. Jule A. RABÓ, Union Carbide Corporation Tarrytown Technical Center,
Old Saw Mill River Road at Route 100C, Tarrytown, New
York 10591, USA